Published in final edited form as:

Hepatology. 2016 August ; 64(2): 488–500. doi:10.1002/hep.28574.

Metallothionein-1G Facilitates Sorafenib Resistance through Inhibition of Ferroptosis

Xiaofang Sun[1], **Xiaohua Niu**[1], **Ruochan Chen**[2], **Wenyin He**[1], **De Chen**[1], **Rui Kang**[2], and **Daolin Tang**[2,*]

[1]The Center for DAMP Biology, The Third Affiliated Hospital of Guangzhou Medical University, Guangzhou, Guangdong, 510510, China

[2]Department of Surgery, University of Pittsburgh Cancer Institute, University of Pittsburgh, Pittsburgh, Pennsylvania 15213, USA

Abstract

Hepatocellular carcinoma (HCC) is a major cause of cancer-related death worldwide and currently has the fastest rising incidence of all cancers. Sorafenib was originally identified as an inhibitor of multiple oncogenic kinases and remains the only approved systemic therapy for advanced HCC. However, acquired resistance to sorafenib has been found in HCC patients, which results in poor prognosis. Here, we showed that metallothionein (MT)-1G is a critical regulator and promising therapeutic target of sorafenib resistance in human HCC cells. The mRNA and protein expression of MT-1G is remarkably induced by sorafenib, but not other clinically-relevant kinase inhibitors (e.g., erlotinib, gefitinib, tivantinib, vemurafenib, selumetinib, imatinib, masitinib, and ponatinib). Activation of transcription factor nuclear factor erythroid 2-related factor 2 (NRF2), but not p53 and hypoxia-inducible factor 1-alpha (HIF1α), is essential for induction of MT-1G expression following sorafenib treatment. Importantly, genetic and pharmacological inhibition of MT-1G enhances the anticancer activity of sorafenib *in vitro* and in tumor xenograft models. The molecular mechanisms underlying the action of MT-1G in sorafenib resistance involves the inhibition of ferroptosis, a novel form of regulated cell death. Knockdown of MT-1G by RNAi increases glutathione depletion and lipid peroxidation, which contributes to sorafenib-induced ferroptosis.

Conclusion—These findings demonstrate a novel molecular mechanism of sorafenib resistance and also suggest that MT-1G is a new regulator of ferroptosis in HCC cells.

Keywords

sorafenib; metallothionein; ferroptosis; hepatocellular carcinoma

Introduction

Hepatocellular carcinoma (HCC), the most common type of liver cancer, is the second leading cause of cancer-related death worldwide, especially in developing countries. The

Correspondence to: Daolin Tang (tangd2@upmc.edu).

Conflict of Interest: The authors declare no conflicts of interest or financial interests.

incidence of HCC is increasing in developed countries (including the United States and countries in Europe) because of the progression of old hepatitis C viral infections, alcohol consumption, the almost epidemic prevalence of obesity, and metabolic syndrome-associated non-alcoholic fatty liver disease (1). The management of HCC has changed significantly in the past few decades with curative options such as hepatic resection, liver transplantation, targeted chemotherapy through the hepatic artery, and systemic therapies (2).

Sorafenib was the first and remains the only approved systemic therapy for advanced HCC patients who are unsuitable for surgical resection (3). The antitumor efficiency of sorafenib correlates with the inhibition of the Ser/Thr kinase Raf and several receptor tyrosine kinases, including vascular endothelial growth factor receptor and epidermal growth factor receptor. In two randomized phase III clinical trials of advanced HCC patients (4, 5), sorafenib treatment improved the time to progression and extended overall survival by 2.8 and 2.3 months compared to the placebo group. The limited survival benefit from these clinical trials suggests the existence of primary and acquired sorafenib resistance mechanisms in HCC cells.

Metallothioneins (MTs) are low molecular weight and cysteine-rich proteins that are highly induced in response to different environmental stressors including metal ions, cytokines, and free radicals (6). MTs play a critical role in heavy metal detoxification and antioxidants. Mammalian MTs have four major members: MT-1, MT-2, MT-3, and MT-4. MT-1 and MT-2 are ubiquitously expressed, including in the liver, whereas MT-3 and MT-4 are expressed mostly in brain tissue and squamous epithelial cells, respectively. Although the MT-2, MT-3, and MT-4 proteins are encoded by a single gene, the MT-1 protein comprises many subtypes encoded by a set of 13 MT-1 genes. The known active MT-1 genes are MT-1A,-1B, -1E, -1F, -1G, -1H, -1M, and -1X. The rest of the MT-1 genes (MT-1C,-1D,-1I, -1J, and 1L) are pseudogenes that are not expressed in humans.

Although increasing evidence indicates that MT expression is a prognostic factor for tumor progression and drug resistance in a variety of malignancies (7–9), the expression and role of MTs in the antitumor activity of sorafenib in HCC cells remains obscure. In this study, we demonstrated that upregulation of MT-1G (but not other MTs) contributes to sorafenib resistance through inhibition of ferroptosis, a recently-recognized form of non-apoptotic regulated cell death (10, 11). Moreover, inhibition of MT-1G expression and activity *in vitro* and *in vivo* enhances the anticancer activity of sorafenib in HCC cells. Collectively, our findings not only identify a novel mechanism of sorafenib resistance, but also suggest a new link between MT-1G and ferroptosis.

Materials and Methods

Antibodies and reagents

The antibody to MT-1G (#LS-B13009) was obtained from LifeSpan BioSciences (Seattle, WA, USA). The antibody to MT-1A (#H00004489-B01P) was obtained from NOVUS (Littleton, CO, USA). The antibody to actin (#3700) was obtained from Cell Signaling Technology (Danvers, MA, USA). The antibody to NRF2 (#ab62352) was obtained from Abcam (Cambridge, MA, USA). Z-VAD-FMK (#V116), cisplatin (#C2210000), all-trans

retinoic acid (ATRA) (#R2625), propargylglycine (PPG) (#P7888), and trigonelline (#T5509) were obtained from Sigma (St. Louis, MO, USA). Necrosulfonamide (#480073) was obtained from EMD Millipore Corporation (Darmstadt, Germany). Erlotinib (#S1023), gefitinib (#S1025), tivantinib (#S2753), vemurafenib (#S1267), selumetinib (#S1008), imatinib (#S1026), masitinib (#S1064), ponatinib (#S1490), erastin (#E7781), sorafenib (#S7397), ferrostatin-1 (#S7243), and liproxstatin-1 (#S7699) were obtained from Selleck Chemicals (Houston, TX, USA). Brusatol (#B250094) was obtained from BePharm (Shanghai, China).

Cell culture

HepaG2 (#HB-8065) and Hep3B (#HB-8064) cells were obtained from American Type Culture Collection. Huh7 cells were a gift from Dr. Allan Tsung (University of Pittsburgh) (12). These cells were grown in Eagle's Minimum Essential Medium (HepaG2 and Hep3B) or Dulbecco's Modified Eagle's Medium (Huh7) with 10% fetal bovine serum, 2 mM L-glutamine, and 100 U/ml of penicillin and streptomycin.

Human hepatocyte isolation

Hepatocytes were isolated from tissue taken from HCC patients who had undergone hepatic resections. Collection of the samples from the Third Affiliated Hospital of Guangzhou Medical University was approved by the Institutional Review Board. Hepatocyte isolation was carried out using a modified “two-stage” collagenase procedure developed by Berry and Friend (13, 14).

Cell viability assay

Cell viability was evaluated using a Cell Counting Kit-8 (#96992, Sigma) according the manufacturer’s instructions. Average percentage of inhibition at each concentration was calculated.

Survival clonogenic assay

Long-term cell survival was monitored in a colony formation assay. In brief, 1,000 cells were treated with individual chemotherapeutic drugs for 24 h and plated into 24-well plates. Colonies were visualized by crystal violet staining two weeks later as previously described (15).

Western blot analysis

Western blot was used to analyze protein expression as described previously (16). In brief, after extraction, proteins in cell lysates were first resolved by SDS-polyacrylamide gel electrophoresis and then transferred to polyvinylidene difluoride membrane and subsequently incubated with the primary antibody. After incubation with peroxidase-conjugated secondary antibodies, the signals were visualized by enhanced chemiluminescence (Pierce, Rockford, IL, USA, #32106) according to the manufacturer's instructions.

RNAi

The human NRF2-shRNA (SHCLNG-NM_006164_TRCN0000007558; Sequence: CCGGCCGGCATTTCACTAAACACAACTCGAGTTGTGTTTAGTGAAATGCCGGTTTTT); human p53-shRNA (SHCLND-NM_000546_TRCN0000003753; Sequence: CCGGCGGCGCACAGAGGAAGAGAATCTCGAGATTCTCTTCCTCTGTGCGCCGTTTTT); human HIF1α-shRNA (SHCLND-NM_001530_TRCN0000003810; Sequence: CCGGGTGATGAAAGAATTACCGAATCTCGAGATTCGGTAATTCTTTCATCACTTTTT); human MT-1G-shRNA_1 (SHCLND-NM_005950_TRCN0000242864; Sequence:CCGGCTCCTGTGCCGCTGGTGTCTCCTCGAGGAGACACCAGCGGCACAGGAGTTTTTG); human MT-1G-shRNA_2 (SHCLND-NM_005950_TRCN0000242865; Sequence: CCGGCCTGCAAGAAGAGCTGCTGCTCTCGAGAGCAGCAGCTCTTCTTGCAGGTTTTTG); and control shRNA were obtained from Sigma. Transfections were performed with Lipofectamine™ 3000 (#L3000008, Invitrogen) according the manufacturer's instructions.

Quantitative real time polymerase chain reaction

Total RNA isolation and quantitative RT-PCR (Q-PCR) were carried out using previously-described procedures (17). Briefly, first-strand cDNA synthesis was carried out by using a Reverse Transcription System Kit according to the manufacturer's instructions (#11801-025, OriGene Technologies, Rockville, MD, USA). cDNA from various cell samples was amplified with specific primers (human MT-1A: 5'- AGAGTGCAAATGCACCTCCTGC-3' and 5'- CGGACATCAGGCACAGCAGCT-3'; human MT-1G: 5'-AGAGTGCAAATGCACCTCCTGC-3' and 5'- TTGTACTTGGGAGCAGGGCTGT-3'; human MT-1B: 5'- GCTTGTCTTGGCTCCACA -3' and 5'-AGCAAACCGGTCAGGTAGTTA-3'; human MT-1E: 5'-ATCCTCTGGGTCTGGGTTCT-3' and 5'- CAGGTTGTGCAGGTTGTTCTA-3'; human MT-1F: 5'- AGTCTCTCCTCGGCTTGC -3' and 5'- ACATCTGGGAGAAAGGTTGTC -3'; human MT-1H: 5'- GCAAATGCACCTCCTGCAAGAAG-3' and 5'-CCGACATCAGGCACAGCAGCT-3'; human MT-1M: 5'- GGGCCTAGCAGTCG -3' and 5'- TGGCTCAGTATCGTATTG -3'; human MT-1X: 5'-AGAGTGCAAATGCACCTCCTGC-3' and 5'- TGTCCTGGCATCAGGCACAGC-3'; human MT-2A: 5'- GAGTGCAAATGCACTTCGTGCAA -3' and 5'-GCGTTCTTTACATCTGGGAGCG -3'; human p53: 5'-CCTCAGCATCTTATCCGAGTGG -3' and 5'- TGGATGGTGGTACAGTCAGAGC -3'; human p21: 5'- AGGTGGACCTGGAGACTCTCAG -3' and 5'-TCCTCTTGGAGAAGATCAGCCG -3'; human NRF2: 5'-CACATCCAGTCAGAAACCAGTGG-3' and 5'-GGAATGTCTGCGCCAAAAGCTG-3'; human HIF1α: 5'- TATGAGCCAGAAGAACTTTTAGGC-3' and 5'-CACCTCTTTTGGCAAGCATCCTG-3'; human glucose transporter 1 (GLUT1): 5'-TTGCAGGCTTCTCCAACTGGAC-3' and 5'- CAGAACCAGGAGCACAGTGAAG-3'; human ferritin heavy chain 1 (FTH1): 5'- TGAAGCTGCAGAACCAACGAGG-3' and 5'-GCACACTCCATTGCATTCAGCC-3'; human transferrin receptor protein 1 (TFR1): 5'-ATCGGTTGGTGCCACTGAATGG-3' and 5'- ACAACAGTGGGCTGGCAGAAAC-3'; human divalent metal transporter 1 (DMT1): 5'- AGCTCCACCATGACAGGAACCT-3' and 5'- TGGCAATAGAGCGAGTCAGAACC-3'; and human prostaglandin-endoperoxide

synthase 2 (PTGS2): 5'- CGGTGAAACTCTGGCTAGACAG-3' and 5'-GCAAACCGTAGATGCTCAGGGA-3') and the data was normalized to actin RNA (human: 5'-CACCATTGGCAATGAGCGGTTC -3' and 5'-AGGTCTTTGCGGATGTCCACGT -3').

Iron assay

The relative iron concentration in cell lysates was assessed using an Iron Assay Kit (#ab83366, Abcam) according the manufacturer's instructions.

Lipid peroxidation assay

The relative malondialdehyde (MDA) concentration in cell lysates was assessed using a Lipid Peroxidation Assay Kit (#ab118970, Abcam) according the manufacturer's instructions.

Glutathione assay

The relative glutathione (GSH) concentration in cell or tissue lysates was assessed using a Glutathione Assay Kit (#CS0260, Sigma) according the manufacturer's instructions.

NRF2 transcriptional activity assay

The transcriptional activity of NRF2 was assayed using a Cignal Antioxidant Response Reporter (luc) Kit (#CCS-5020L, Qiagen) according the manufacturer's instructions.

Animal models

All animal experiments were approved by the Third Affiliated Hospital of Guangzhou Medical University and the University of Pittsburgh Institutional Animal Care and Use Committees and performed in accordance with the Association for Assessment and Accreditation of Laboratory Animal Care guidelines (http://www.aaalac.org).

To generate murine subcutaneous tumors, 2×10^6 Huh7 cells in control shRNA or MT-1G knockdown cells in 200 μl phosphate buffered saline were injected subcutaneously to the right of the dorsal midline in nude mice. Once the tumors reached 80–100 mm^3 at day seven, mice were randomly allocated into groups and treated with sorafenib (10 mg/kg/ intraperitoneal injection (i.p.), once every other day) for two weeks. On day 22 after the start of treatment, tumors were removed. Tumors were measured twice weekly and volumes were calculated using the formula length×$width^2\times\pi/6$.

In another experiment, nude mice were injected subcutaneously with indicated Huh7 cells (2×10^6 cells/mouse) and treated with sorafenib (10 mg/kg/i.p., once every other day) with or without ATRA (0.5 mg/kg/i.p., once every other day) or PPG (10 mg/kg/i.p., once every other day) at day seven for two weeks. On day 22 after the start of treatment, tumors were removed. Tumors were measured twice weekly and volumes were calculated using the formula length×$width^2\times\pi/6$.

Statistical analysis

Data are expressed as means ± SD of three independent experiments. Unpaired Student's t tests were used to compare the means of two groups. One-way ANOVA was used for comparison among the different groups. When the ANOVA was significant, *post hoc* testing of differences between groups was performed using the LSD test. A P-value < 0.05 was considered significant.

Results

Sorafenib induces MT-1G expression in human HCC cells

To determine whether sorafenib induces MT expression, Huh7 (a human HCC cell line) cells were treated with sorafenib for six and 24 hours and the mRNA levels of MT-1A,-1B, -1E, -1F, -1G, -1H, -1M, -1X, and 2A were analyzed via Q-PCR. Among these MTs, MT-1G was the most highly-induced gene following sorafenib treatment (Fig. 1A). In contrast, the mRNA expression of MT-1G was not affected in Huh7 cells following treatment with other tyrosine kinase inhibitors including erlotinib, gefitinib, tivantinib, vemurafenib, selumetinib, imatinib, masitinib, and ponatinib (Fig. 1B). Consistently, western blot analysis revealed that the protein level of MT-1G, but not MT-1A, was significantly increased in Huh7 cells following treatment with sorafenib, but not other tyrosine kinase inhibitors (Fig. 1C). Moreover, sorafenib-induced MT-1G protein expression was observed in other human HCC cell lines (HepaG2 and Hep3B) and primary tumor hepatocytes from HCC patients (Fig. 1D). These data indicate that sorafenib specifically induces MT-1G expression in various human HCC cells.

NRF2 is required for sorafenib-induced MT-1G expression

Previous studies have shown that sorafenib can regulate the activity of distinct transcription factors (e.g., p53 (18), HIF1α (19), and NRF2 (20)) to affect cell death and survival in HCC cells. To determine which transcription factor is required for sorafenib-induced MT-1G expression, target-specific shRNAs against p53 (Fig. 2A), HIF1α (Fig. 2B), and NRF2 (Fig. 2C) were transfected into Huh7 and/or HepG2 cells. The mRNA levels of p53, HIF1α, and NRF2 were not significantly affected by sorafenib (Fig. 2A–C). Interestingly, knockdown of NRF2, but not p53 and HIF1α, significantly inhibited sorafenib-induced MT-1G mRNA expression (Fig. 2A–C). As the positive controls, knockdown of p53 inhibited cisplatin-induced p21 mRNA expression in HepG2 cells (Fig. 2A), whereas knockdown of HIF1α inhibited hypoxia-induced GLUT1 mRNA expression in Huh7 cells (Fig. 2B). Consistent with our previous study (20), sorafenib increased NRF2 expression mainly at the protein level (Fig. 2D), but not the mRNA level (Fig. 2C). Knockdown of NRF2 also suppressed sorafenib-induced MT-1G protein expression in Huh7 and HepG2 cells (Fig. 2D). Moreover, potent NRF2 inhibitors (e.g., ATRA (21), trigonelline (22), and brusatol (23)) limited sorafenib-induced NRF2 transcriptional activity (Fig. 2E) and MT-1G expression (Fig. 2F) in Huh7 cells. PPG, an irreversible inhibitor of cystathionase (24), was used to inhibit the synthesis of MTs in previous reports. PPG also inhibited sorafenib-induced NRF2 transcriptional activity (Fig. 2E) and MT-1G expression (Fig. 2F) in Huh7 cells. Thus, these findings suggest that activation of NRF2 via the cystathionase pathway is required for sorafenib-induced MT-1G expression in HCC cells.

Suppression of MT-1G expression enhances sorafenib sensitivity

To determine whether increased MT-1G expression regulates the anticancer activity of sorafenib, two different shRNAs targeting MT-1G were transfected into Huh7 and HepG2 cells. Indeed, suppression of MT-1G expression by RNAi (Fig. 3A) significantly enhances sorafenib-induced cell death at 48 hours as shown by cell viability assay (Fig. 3B). Colony formation assay also indicated that suppression of MT-1G expression inhibited long-term HCC cell proliferation following sorafenib treatment (Fig. 3C). Both NRF2 inhibitors (e.g., ATRA, trigonelline, and brusatol) and PPG enhance sorafenib-induced HCC cell death (Fig. 3D). Collectively, these findings indicate that suppression of MT-1G expression enhances sorafenib antitumor sensitivity in HCC cells.

MT-1G is a negative regulator of ferroptosis in HCC cells

To determine the basis for MT-1G in mediating sorafenib resistance, we treated MT-1G knockdown HCC cells with several potent cell death inhibitors. The ferroptosis inhibitors (ferrostatin-1 (25) and liprostatin-1 (26)) significantly restored cell viability in both control shRNA and MT-1G knockdown cells following sorafenib treatment (Fig. 4A). ZVAD-FMK (an apoptosis inhibitor) and necrosulfonamide (a necroptosis inhibitor) had no influence on sorafenib-induced cell death (Fig. 4A). In contrast, ZVAD-FMK inhibited apoptotic stimuli staurosporine-induced cell death, whereas necrosulfonamide inhibited necroptotic stimuli (TNFα+ZVAD-FMK)-induced cell death (Fig. 4B). Moreover, knockdown of MT-1G also enhanced cell death induced by the classical ferroptotic inducer erastin; this process can by reversed by ferrostatin-1 and liprostatin-1 (but not ZVAD-FMK and necrosulfonamide) (Fig. 4A). These findings suggest that MT-1G is a negative regulator of ferroptosis in HCC cells.

Ferroptosis is characterized by the accumulation of lipid peroxidation products that require abundant and accessible cellular iron (10, 11); thus, we further investigated whether MT-1G is involved in the regulation of lipid peroxidation and iron metabolism leading to sorafenib resistance. The end products of lipid peroxidation, such as MDA, were significantly increased following treatment with erastin and sorafenib in MT-1G knockdown cells (Fig. 4C). As expected, NRF2 inhibitors (e.g., ATRA, trigonelline, and brusatol) and PPG also increased sorafenib- and erastin-induced MDA production (Fig. 4D). Ferrous iron (Fe^{2+}) can participate in Fenton reaction and generate the toxic reactive oxygen species (ROS) to trigger ferroptosis (27). However, knockdown of MT-1G did not significantly affect the levels of Fe^{2+} following treatment with sorafenib or erastin (Fig. 4C). The mRNA levels of iron metabolism genes (e.g., FTH1, TFR1, and DMT1) were not affected by knockdown of MT-1G in Huh7 cells (Fig. 4C). These findings suggest that MT-1G inhibits ferroptosis via modulating lipid peroxidation, but not Fe^{2+} production and metabolism.

In addition to Fe^{2+}-mediated ROS production by Fenton reaction, GSH depletion-mediated lipid peroxidation is implicated in the induction of ferroptosis (25, 28). We found that kncodown of MT-1G remarkably increased intracellular GSH depletion in HCC cells following treatment with sorafenib or erastin (Fig. 4C). Consistently, NRF2 inhibitors (e.g., ATRA, trigonelline, and brusatol) and PPG also increased intracellular GSH depletion in HCC cells following treatment with sorafenib or erastin (Fig. 4D). Thus, these findings

suggest that MT-1G inhibits ferroptosis via blocking GSH depletion-mediated lipid peroxidation, and this process facilities sorafenib resistance in HCC cells.

Targeting MT-1G enhances the anticancer activity of sorafenib in vivo

To determine whether suppression of MT-1G expression enhances anticancer activity of sorafenib *in vivo*, MT-1G knockdown mouse Huh7 cells were implanted into the subcutaneous space of the right flank of nude mice. Beginning at day seven, these mice were treated with sorafenib. Compared with the control shRNA group, sorafenib treatment effectively reduced the size of tumors (Fig. 5A) formed by MT-1G knockdown cells with decreased GSH levels (Fig. 5B) and MT-1G mRNA expression (Fig. 5C). In contrast, the mRNA expression of PTGS2, a marker for assessment of ferroptosis *in vivo* (28), was increased in the MT-1G knockdown group after treatment with sorafenib (Fig. 5C). These findings indicated that the knockdown of MT-1G increases GSH depletion and ferroptosis. Similar to our previous study using trigonelline (20), administration of ATRA or PPG in mice also enhanced the anticancer activity of sorafenib in subcutaneous xenograft models (Fig. 5D). This process was associated with reduced GSH levels (Fig. 5E), decreased MT-1G mRNA (Fig. 5F), and increased PTGS2 mRNA (Fig. 5F) in isolated tumor tissue. These experiments suggest that genetic and pharmacological inhibition of MT-1G expression rendered HCC more sensitive to sorafenib via induction of GSH depletion and ferroptosis *in vivo*.

Discussion

Sorafenib leads to a survival benefit in patients with advanced HCC, but its use is hampered by drug resistance. In this study, we showed that upregulation of MT-1G by activation of NRF2 contributes to sorafenib resistance in human HCC cells. This alteration of MT-1G expression by sorafenib is not dependent on kinase inhibition. Upregulation of MT-1G limits sorafenib-induced lipid peroxidation and subsequent ferroptosis. Thus, blocking MT-1G expression enhances the anticancer activity of sorafenib by induction of ferroptosis *in vitro* and *in vivo*.

MTs are small proteins with a high affinity for divalent heavy metal ions that play an important role in the protection against heavy metals and oxidative injury. Like oxidative stress, MTs have been suggested to act as an oncogene or tumor suppressor, depending on the tumor type and stage. Previous studies have shown that MT-1, as well as MT-1G expression, was repressed by promoter methylation in several human cancers, including HCC (29, 30). Double knockout of MT-1 and MT-2 promotes diethylnitrosamine-induced hepatocarcinogenesis by activation of superoxide production in mice, suggesting that MTs play a tumor suppressor role in tumorigenesis (31). Our current study showed that the expression of MT-1G (but not other MTs) is specifically upregulated in HCC cells in response to sorafenib. In contrast, other tyrosine kinase inhibitors cannot induce MT-1G expression. Importantly, increased MT-1G expression in HCC cells facilities sorafenib resistance, suggesting a pro-survival role in tumor therapy. Thus, MT-1G seems to play a dual role in HCC. On one hand, expression of the MT-1G is critical for ameliorating or eliminating heavy metals and free radicals to maintain cellular redox homeostasis. As a

result, activation of MT-1G expression may be a strategy for HCC prevention. On the other hand, MT-1G is upregulated in resistant cancer cells and is thought to be responsible for acquired chemoresistance (32). Therefore, it may be necessary to inhibit the MT-1G pathway during sorafenib-mediated chemotherapy.

Our current data indicated that MT-1G is a novel transcriptional target of NRF2, but not p53 and HIF1α. NRF2 is a basic leucine zipper transcription factor that regulates redox balance and the stress response triggered by injury and inflammation (33). Under unstressed conditions, Kelch-like ECH-associated protein 1 (Keap1) constitutively ubiquitinates NRF2, resulting in the rapid degradation of NRF2 through the proteasome pathway, thus maintaining a low level of cellular NRF2. Under stressed conditions (e.g., oxidative stress), inducers modify the Keap1 cysteines or expression leading to NRF2 stabilization (34). We previously demonstrated that sorafenib prevented NRF2 degradation and enhanced subsequent NRF2 nuclear accumulation through inactivation of Keap1 (20). Associated with this, sorafenib-induced HCC cell death depends on ROS production. Our current study showed that genetic or pharmacologic inhibition of NRF2 significantly inhibited MT-1G expression and increased ROS production in HCC cells following sorafenib treatment.

Importantly, MT-1G-mediated sorafenib resistance occurs through the inhibition of ferroptosis, a form of regulated cell death recently recognized in 2012 (25). Ferroptosis is remarkably distinct from other types of regulated cell death such as apoptosis and necroptosis. For example, the classic biochemical features of apoptosis (e.g., caspase activation and poly ADP ribose polymerase cleavage) and necroptosis (e.g., receptor-interacting protein kinase 1/3 activation) are not observed in ferroptosis (25). In contrast, ferroptosis is characterized by the accumulation of ROS from iron metabolism and lipid peroxidation (25), although the downstream effector proteins mediating these effects remain unknown (11). In addition to cancer therapy (28), impaired ferroptosis also involves tissue injury (26, 35), immunity tolerance (36), and stem cell division (37).

Interestingly, we and others have recently demonstrated that sorafenib is a strong inducer of ferroptosis, but not apoptosis, in HCC cells (20, 38, 39). Sorafenib-induced ferroptosis is independent of the status of oncogenes (e.g., Ras, Raf, and PIK3CA) (40) and kinase inhibition (41). Several genes or proteins responsible for the regulation of iron metabolism and lipid peroxidation have been involved in ferroptosis. For example, glutathione peroxidase 4 (28) and heat shock protein beta-1 (42) inhibit ferroptosis by limiting lipid peroxidation and reducing cellular iron uptake, respectively. In contrast, p53 (especially acetylation-defective mutant p53) (43) and cysteinyl-tRNA synthetase (44) promote ferroptosis by inhibiting expression of SLC7A11 (a specific light chain subunit of cystine/glutamate antiporter) and transsulfuration pathway, respectively. In the current study, we demonstrated that upregulated MT-1G inhibits lipid peroxidation without altering iron levels in HCC cells. Knockdown of MT-1G results in GSH depletion and lipid peroxidation in response to sorafenib as well as erastin. MT-1G might regulate depletion of GSH through modulation of GSH biosynthetic enzymes (45). Furthermore, ferroptosis inhibitors (but not other cell death inhibitors) reverted the MT-1G knockdown-mediated phenotypes in response to sorafenib and erastin. Unlike sorafenib and erastin, RSL3 was found to directly

bind GPX4 and inactivate its peroxidase activity (28). It remains unknown whether MT-1G affects RSL3-induced ferroptosis.

In addition to MT-1G, upregulation of other NRF2 target genes including quinone oxidoreductase 1, heme oxygenase-1, and FTH1 also inhibit sorafenib-induced ferroptosis (46). These data thus suggest that NRF2 is a master transcription factor involved in blocking sorafenib-induced ferroptosis by regulating the genes involved in redox and iron metabolism.

In summary, the regulation of cell death is an important factor in both tumor development and responses to anticancer therapies (47). We demonstrated that upregulated MT-1G expression protects HCC cells from sorafenib and facilitates cancer progression by inhibition of lipid peroxidation-mediated ferroptosis. Notably, inhibition of MT-1G expression by RNAi or administration of ATRA or PPG significantly enhanced the anticancer activity of sorafenib in xenograft tumor models. Thus, modulation of MT-1G expression is a potential therapeutic strategy to overcome acquired resistance to sorafenib in HCC cells.

Acknowledgments

We thank Christine Heiner (Department of Surgery, University of Pittsburgh) for her critical reading of the manuscript.

Financial Support: This work was supported by the National Institutes of Health (R01CA160417 and R01GM115366 to D.T.), the National Natural Science Foundation of China (31171229 and U1132005, to X.S.; 81502445 to X.N.), and a Science of Guangzhou Key Project (201508020258 and 201400000003/4, to X.S.). This project partly used University of Pittsburgh Cancer Institute shared resources supported by award P30CA047904.

List of Abbreviations

HCC	hepatocellular carcinoma
MT	metallothionein
Q-PCR	quantitative RT-PCR
MDA	malondialdehyde
GSH	glutathione
GLUT1	glucose transporter 1
ATRA	all-trans retinoic acid
PPG	propargylglycine
FTH1	ferritin heavy chain 1
TFR1	transferrin receptor protein 1
DMT1	divalent metal transporter 1
PTGS2	prostaglandin-endoperoxide synthase 2

Keap1	Kelch-like ECH-associated protein 1
ROS	reactive oxygen species
NRF2	nuclear factor erythroid 2-related factor 2
HIF1α	hypoxia-inducible factor 1-alpha
i.p.	intraperitoneal injection

References

1. Siegel RL, Miller KD, Jemal A. Cancer statistics, 2016. CA: a cancer journal for clinicians. 2016; 66:7–30. [PubMed: 26742998]
2. El-Serag HB. Hepatocellular carcinoma. The New England journal of medicine. 2011; 365:1118–1127. [PubMed: 21992124]
3. Siegel AB, Olsen SK, Magun A, Brown RS Jr. Sorafenib: where do we go from here? Hepatology. 2010; 52:360–369. [PubMed: 20578152]
4. Llovet JM, Ricci S, Mazzaferro V, Hilgard P, Gane E, Blanc JF, et al. Sorafenib in advanced hepatocellular carcinoma. N Engl J Med. 2008; 359:378–390. [PubMed: 18650514]
5. Cheng AL, Kang YK, Chen Z, Tsao CJ, Qin S, Kim JS, et al. Efficacy and safety of sorafenib in patients in the Asia-Pacific region with advanced hepatocellular carcinoma: a phase III randomised, double-blind, placebo-controlled trial. Lancet Oncol. 2009; 10:25–34. [PubMed: 19095497]
6. Coyle P, Philcox JC, Carey LC, Rofe AM. Metallothionein: the multipurpose protein. Cellular and molecular life sciences : CMLS. 2002; 59:627–647. [PubMed: 12022471]
7. Chun JH, Kim HK, Kim E, Kim IH, Kim JH, Chang HJ, et al. Increased expression of metallothionein is associated with irinotecan resistance in gastric cancer. Cancer research. 2004; 64:4703–4706. [PubMed: 15256434]
8. Gumulec J, Raudenska M, Adam V, Kizek R, Masarik M. Metallothionein - immunohistochemical cancer biomarker: a meta-analysis. PloS one. 2014; 9:e85346. [PubMed: 24416395]
9. Eckschlager T, Adam V, Hrabeta J, Figova K, Kizek R. Metallothioneins and cancer. Current protein & peptide science. 2009; 10:360–375. [PubMed: 19689357]
10. Yang WS, Stockwell BR. Ferroptosis: Death by Lipid Peroxidation. Trends in cell biology. 2015
11. Xie Y, Hou W, Song X, Yu Y, Huang J, Sun X, et al. Ferroptosis: process and function. Cell death and differentiation. 2016
12. Yan W, Chang Y, Liang X, Cardinal JS, Huang H, Thorne SH, et al. High-mobility group box 1 activates caspase-1 and promotes hepatocellular carcinoma invasiveness and metastases. Hepatology. 2012; 55:1863–1875. [PubMed: 22234969]
13. Berry MN, Friend DS. High-yield preparation of isolated rat liver parenchymal cells: a biochemical and fine structural study. The Journal of cell biology. 1969; 43:506–520. [PubMed: 4900611]
14. Lecluyse EL, Alexandre E. Isolation and culture of primary hepatocytes from resected human liver tissue. Methods Mol Biol. 2010; 640:57–82. [PubMed: 20645046]
15. Wang P, Yu J, Zhang L. The nuclear function of p53 is required for PUMA-mediated apoptosis induced by DNA damage. Proc Natl Acad Sci U S A. 2007; 104:4054–4059. [PubMed: 17360476]
16. Tang D, Kang R, Livesey KM, Kroemer G, Billiar TR, Van Houten B, et al. High-mobility group box 1 is essential for mitochondrial quality control. Cell Metab. 2011; 13:701–711. [PubMed: 21641551]
17. Yang L, Xie M, Yang M, Yu Y, Zhu S, Hou W, et al. PKM2 regulates the Warburg effect and promotes HMGB1 release in sepsis. Nature communications. 2014; 5:4436.
18. Wei JC, Meng FD, Qu K, Wang ZX, Wu QF, Zhang LQ, et al. Sorafenib inhibits proliferation and invasion of human hepatocellular carcinoma cells via up-regulation of p53 and suppressing FoxM1. Acta pharmacologica Sinica. 2015; 36:241–251. [PubMed: 25557114]

19. Liang Y, Zheng T, Song R, Wang J, Yin D, Wang L, et al. Hypoxia-mediated sorafenib resistance can be overcome by EF24 through Von Hippel-Lindau tumor suppressor-dependent HIF-1alpha inhibition in hepatocellular carcinoma. Hepatology. 2013; 57:1847–1857. [PubMed: 23299930]
20. Sun X, Ou Z, Chen R, Niu X, Chen D, Kang R, et al. Activation of the p62-Keap1-NRF2 pathway protects against ferroptosis in hepatocellular carcinoma cells. Hepatology. 2016; 63:173–184. [PubMed: 26403645]
21. Wang XJ, Hayes JD, Henderson CJ, Wolf CR. Identification of retinoic acid as an inhibitor of transcription factor Nrf2 through activation of retinoic acid receptor alpha. Proceedings of the National Academy of Sciences of the United States of America. 2007; 104:19589–19594. [PubMed: 18048326]
22. Arlt A, Sebens S, Krebs S, Geismann C, Grossmann M, Kruse ML, et al. Inhibition of the Nrf2 transcription factor by the alkaloid trigonelline renders pancreatic cancer cells more susceptible to apoptosis through decreased proteasomal gene expression and proteasome activity. Oncogene. 2013; 32:4825–4835. [PubMed: 23108405]
23. Ren D, Villeneuve NF, Jiang T, Wu T, Lau A, Toppin HA, et al. Brusatol enhances the efficacy of chemotherapy by inhibiting the Nrf2-mediated defense mechanism. Proceedings of the National Academy of Sciences of the United States of America. 2011; 108:1433–1438. [PubMed: 21205897]
24. Lertratanangkoon K, Scimeca JM, Wei JN. Inhibition of glutathione synthesis with propargylglycine enhances N-acetylmethionine protection and methylation in bromobenzene-treated Syrian hamsters. The Journal of nutrition. 1999; 129:649–656. [PubMed: 10082769]
25. Dixon SJ, Lemberg KM, Lamprecht MR, Skouta R, Zaitsev EM, Gleason CE, et al. Ferroptosis: an iron-dependent form of nonapoptotic cell death. Cell. 2012; 149:1060–1072. [PubMed: 22632970]
26. Friedmann Angeli JP, Schneider M, Proneth B, Tyurina YY, Tyurin VA, Hammond VJ, et al. Inactivation of the ferroptosis regulator Gpx4 triggers acute renal failure in mice. Nature cell biology. 2014; 16:1180–1191. [PubMed: 25402683]
27. Dixon SJ, Stockwell BR. The role of iron and reactive oxygen species in cell death. Nature chemical biology. 2014; 10:9–17. [PubMed: 24346035]
28. Yang WS, SriRamaratnam R, Welsch ME, Shimada K, Skouta R, Viswanathan VS, et al. Regulation of ferroptotic cancer cell death by GPX4. Cell. 2014; 156:317–331. [PubMed: 24439385]
29. Kanda M, Nomoto S, Okamura Y, Nishikawa Y, Sugimoto H, Kanazumi N, et al. Detection of metallothionein 1G as a methylated tumor suppressor gene in human hepatocellular carcinoma using a novel method of double combination array analysis. International journal of oncology. 2009; 35:477–483. [PubMed: 19639168]
30. Datta J, Majumder S, Kutay H, Motiwala T, Frankel W, Costa R, et al. Metallothionein expression is suppressed in primary human hepatocellular carcinomas and is mediated through inactivation of CCAAT/enhancer binding protein alpha by phosphatidylinositol 3-kinase signaling cascade. Cancer research. 2007; 67:2736–2746. [PubMed: 17363595]
31. Majumder S, Roy S, Kaffenberger T, Wang B, Costinean S, Frankel W, et al. Loss of metallothionein predisposes mice to diethylnitrosamine-induced hepatocarcinogenesis by activating NF-kappaB target genes. Cancer research. 2010; 70:10265–10276. [PubMed: 21159647]
32. Bahnson RR, Basu A, Lazo JS. The role of metallothioneins in anticancer drug resistance. Cancer treatment and research. 1991; 57:251–260. [PubMed: 1686720]
33. Ma Q. Role of nrf2 in oxidative stress and toxicity. Annu Rev Pharmacol Toxicol. 2013; 53:401–426. [PubMed: 23294312]
34. Suzuki T, Motohashi H, Yamamoto M. Toward clinical application of the Keap1-Nrf2 pathway. Trends Pharmacol Sci. 2013; 34:340–346. [PubMed: 23664668]
35. Linkermann A, Skouta R, Himmerkus N, Mulay SR, Dewitz C, De Zen F, et al. Synchronized renal tubular cell death involves ferroptosis. Proceedings of the National Academy of Sciences of the United States of America. 2014; 111:16836–16841. [PubMed: 25385600]
36. Matsushita M, Freigang S, Schneider C, Conrad M, Bornkamm GW, Kopf M. T cell lipid peroxidation induces ferroptosis and prevents immunity to infection. The Journal of experimental medicine. 2015; 212:555–568. [PubMed: 25824823]

37. Gascon S, Murenu E, Masserdotti G, Ortega F, Russo GL, Petrik D, et al. Identification and Successful Negotiation of a Metabolic Checkpoint in Direct Neuronal Reprogramming. Cell stem cell. 2015

38. Louandre C, Ezzoukhry Z, Godin C, Barbare JC, Maziere JC, Chauffert B, et al. Iron-dependent cell death of hepatocellular carcinoma cells exposed to sorafenib. International journal of cancer Journal international du cancer. 2013; 133:1732–1742. [PubMed: 23505071]

39. Galmiche A, Chauffert B, Barbare JC. New biological perspectives for the improvement of the efficacy of sorafenib in hepatocellular carcinoma. Cancer letters. 2014; 346:159–162. [PubMed: 24380851]

40. Lachaier E, Louandre C, Godin C, Saidak Z, Baert M, Diouf M, et al. Sorafenib induces ferroptosis in human cancer cell lines originating from different solid tumors. Anticancer research. 2014; 34:6417–6422. [PubMed: 25368241]

41. Dixon SJ, Patel DN, Welsch M, Skouta R, Lee ED, Hayano M, et al. Pharmacological inhibition of cystine-glutamate exchange induces endoplasmic reticulum stress and ferroptosis. eLife. 2014; 3:e02523. [PubMed: 24844246]

42. Sun X, Ou Z, Xie M, Kang R, Fan Y, Niu X, et al. HSPB1 as a novel regulator of ferroptotic cancer cell death. Oncogene. 2015; 34:5617–5625. [PubMed: 25728673]

43. Jiang L, Kon N, Li T, Wang SJ, Su T, Hibshoosh H, et al. Ferroptosis as a p53-mediated activity during tumour suppression. Nature. 2015; 520:57–62. [PubMed: 25799988]

44. Hayano M, Yang WS, Corn CK, Pagano NC, Stockwell BR. Loss of cysteinyl-tRNA synthetase (CARS) induces the transsulfuration pathway and inhibits ferroptosis induced by cystine deprivation. Cell death and differentiation. 2016; 23:270–278. [PubMed: 26184909]

45. Ruttkay-Nedecky B, Nejdl L, Gumulec J, Zitka O, Masarik M, Eckschlager T, et al. The role of metallothionein in oxidative stress. International journal of molecular sciences. 2013; 14:6044–6066. [PubMed: 23502468]

46. Sun X, Ou Z, Chen R, Niu X, Chen, Kang R, et al. Activation of the p62-Keap1-NRF2 Pathway Protects against Ferroptosis in Hepatocellular Carcinoma Cells. Hepatology. 2015

47. Conrad M, Angeli JP, Vandenabeele P, Stockwell BR. Regulated necrosis: disease relevance and therapeutic opportunities. Nature reviews Drug discovery. 2016

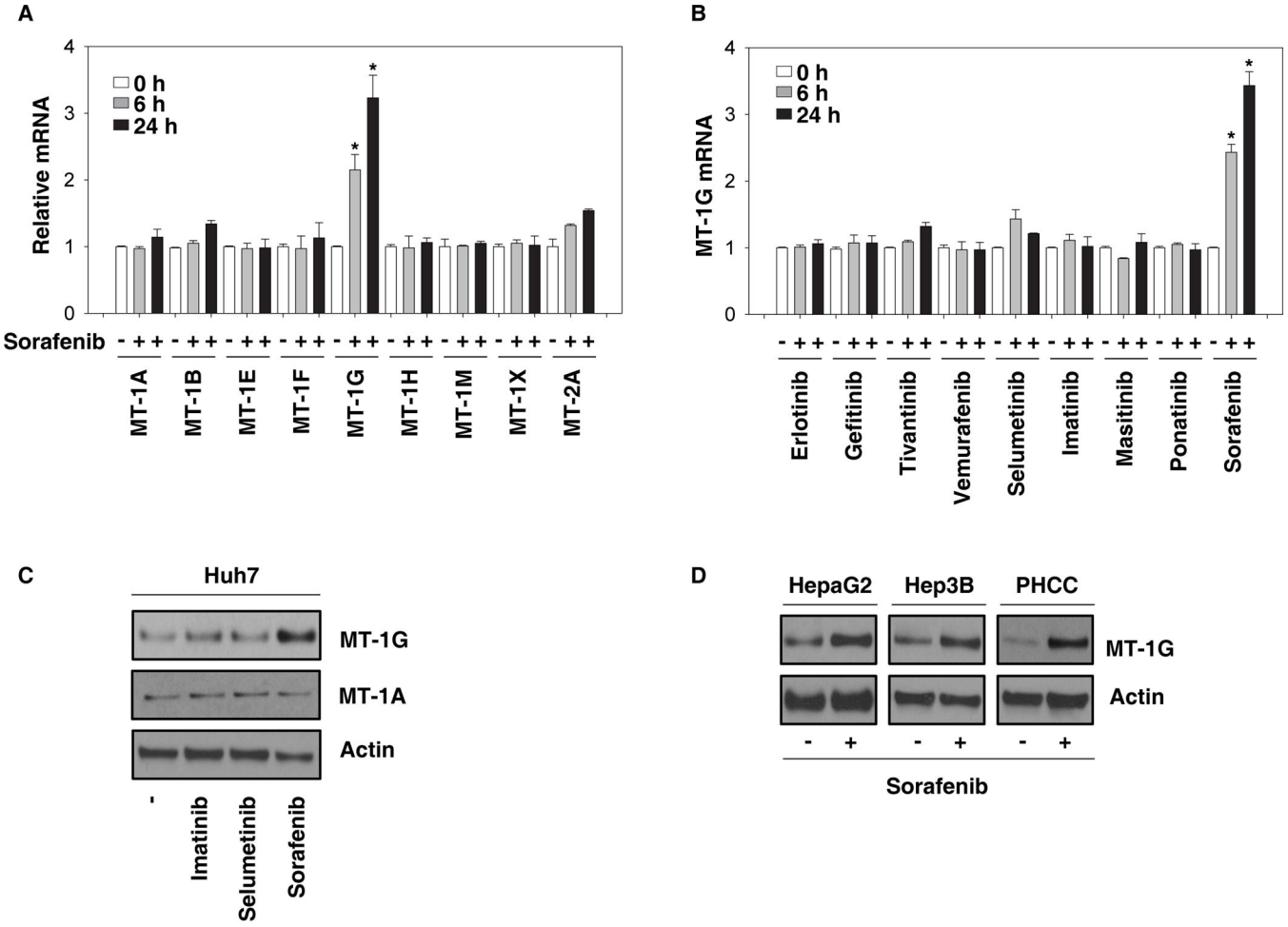

Figure 1. Sorafenib induces MT-1G expression in human hepatocellular carcinoma (HCC cells)

(A, B) Huh7 cells were treated with sorafenib (5 μM) or indicated clinically-relevant kinase inhibitors (5 μM) for 6–24 h and mRNA expressions of indicated metallothioneins (MTs) were assayed by Q-PCR (n=3, *p < 0.05 versus untreated group). (C) Huh7 cells were treated with imatinib (5 μM), selumetinib (5 μM), and sorafenib (5 μM) for 24 h and the protein expression of MT-1G and MT-1A was assayed using western blot. (D) Human HCC cell lines (HepaG2 and Hep3B) and primary tumor hepatocytes from HCC patients (PHCC) were treated with sorafenib (5 μM) for 24 h and the protein expression of MT-1G was assayed by western blot.

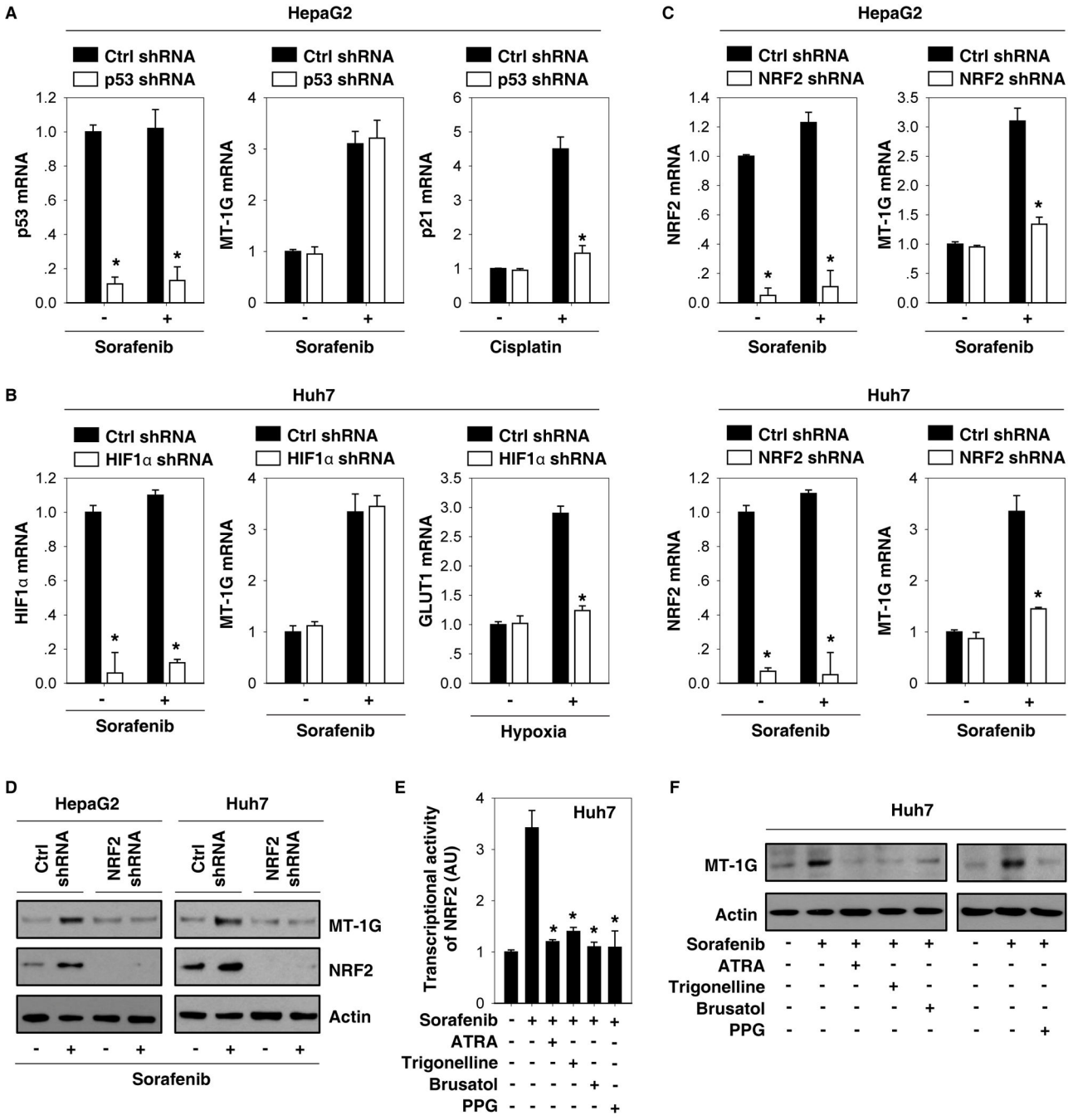

Figure 2. Nuclear factor erythroid 2-related factor 2 (NRF2) is required for sorafenib-induced metallothionein (MT)-1G expression in human hepatocellular carcinoma (HCC) cells

(A–C) Indicated HCC cells were treated with sorafenib (5 μM), cisplatin (25 μM), or hypoxia (1% O_2) for 24 hours and the mRNA levels of indicated genes were assayed using Q-PCR (n=3, *p < 0.05 versus control shRNA group). (D) Knockdown of NRF2 by shRNA inhibited sorafenib-induced MT-1G protein expression by western blot. (E, F) Huh7 cells were treated with sorafenib (5 μM) with or without all-trans retinoic acid (ATRA) (1 μM), trigonelline (0.5 μM), brusatol (40 nM) or propargylglycine (PPG) (2 mM) for 24 hours. The

transcription activity of NRF2 (E) and MT-1G protein expression were assayed (n=3, *p < 0.05 versus sorafenib treatment group).

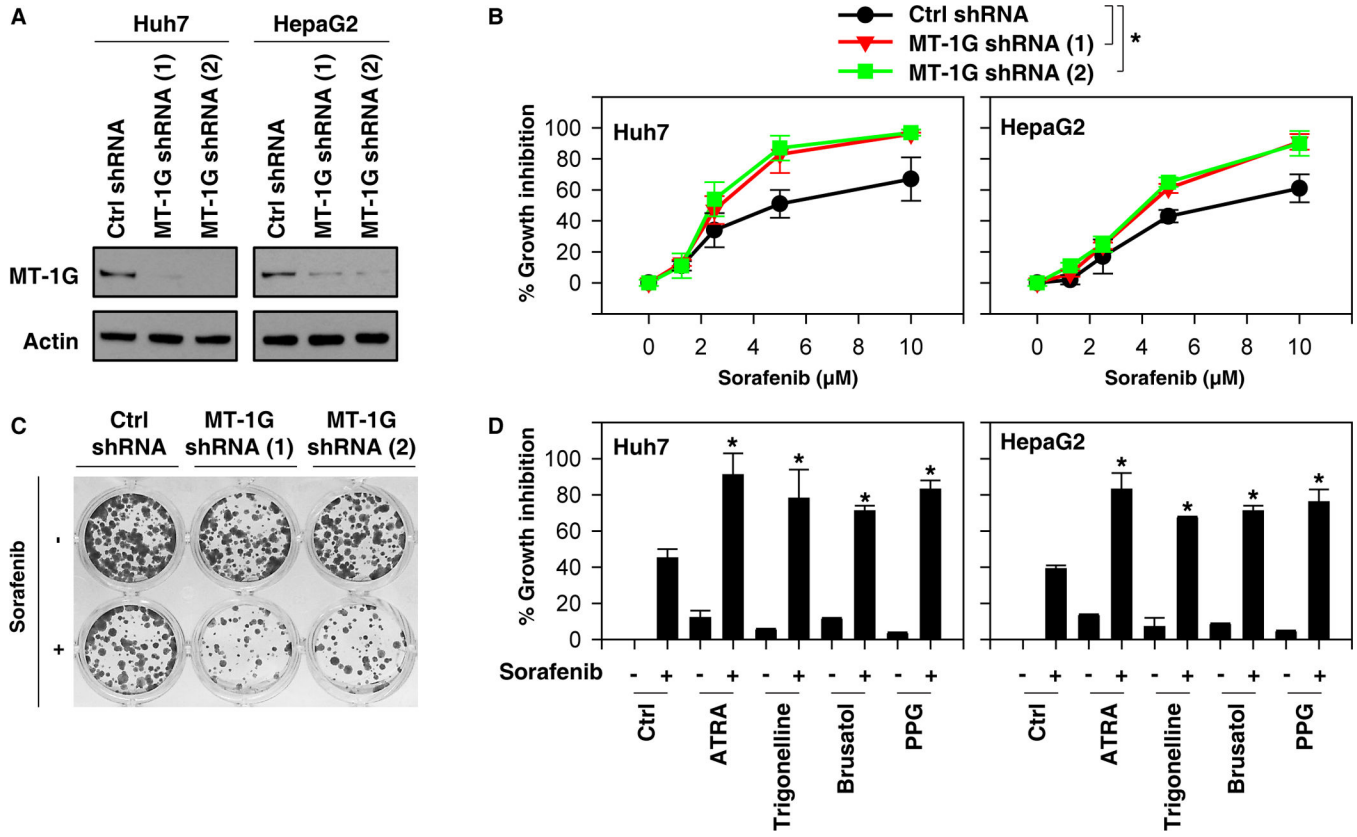

Figure 3. Suppression of metallothionein (MT)-1G expression enhances sorafenib sensitivity

(A) Western blot analysis of MT-1G expression in indicated MT-1G knockdown hepatocellular carcinoma (HCC) cells. (B) Indicated MT-1G knockdown HCC cells were treated with sorafenib (1.25–10 μM) for 24 hours and cell viabilities were assayed (n=3, *p < 0.05). (C) Clonogenic cell survival assay. Indicated Huh7 cells were treated with sorafenib (5 μM) for 24 h, then 1,000 cells were plated into 24-well plates. Colonies were visualized by crystal violet staining two weeks later. (D) Indicated HCC cells were treated with sorafenib (5 μM) with or without all-trans retinoic acid (ATRA) (1 μM), trigonelline (0.5 μM), brusatol (40 nM), or propargylglycine (PPG) (2 mM) for 24 hours and cell viability was assayed (n=3, *p < 0.05 versus control group).

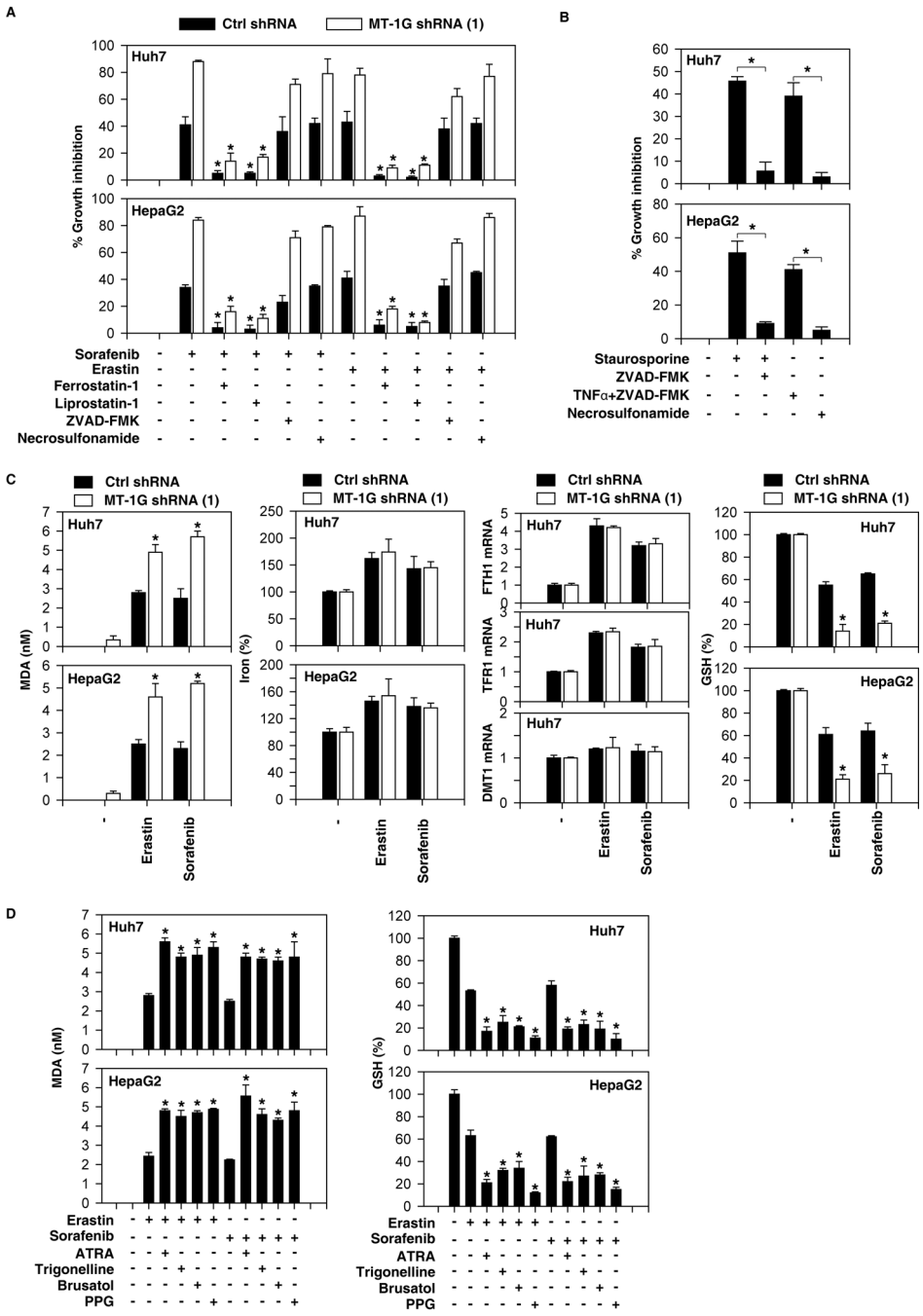

Figure 4. Metallothionein (MT)-1G is a negative regulator of ferroptosis in hepatocellular carcinoma (HCC) cells

(A) Indicated HCC cells were treated with sorafenib (5 μM) and erastin (10 μM) with or without cell death inhibitors (ferrostatin-1, 1 μM; liprostatin-1, 100nM; ZVAD-FMK,10 μM; necrosulfonamide, 0.5 μM) for 24 hours and cell viability was assayed (n=3, *$p < 0.05$ versus sorafenib or erastin treatment group). (B) Indicated HCC cells were treated with apoptosis inducer staurosporine (0.5 μM) or necroptosis inducer (ZVAD-FMK [10 μM]/ TNFα (10 ng/ml) with or without ZVAD-FMK (10 μM) and necrosulfonamide (0.5 μM) for 24 hours and cell viability was assayed (n=3, *$p < 0.05$). (C) Indicated HCC cells were

treated with erastin (10 μM) or sorafenib (5 μM) for 24 hours. The levels of malondialdehyde (MDA), Fe^{2+}, indicated gene mRNA, and glutathione (GSH) levels were assayed (n=3, *p < 0.05 versus control shRNA group). (D) Indicated HCC cells were treated with erastin (10 μM) or sorafenib (5 μM) with or without all-trans retinoic acid (ATRA) (1 μM), trigonelline (0.5 μM), brusatol (40 nM), or propargylglycine (PPG) (2 mM) for 24 hours. The levels of MDA and GSH were assayed (n=3, *p < 0.05 versus sorafenib or erastin treatment group).

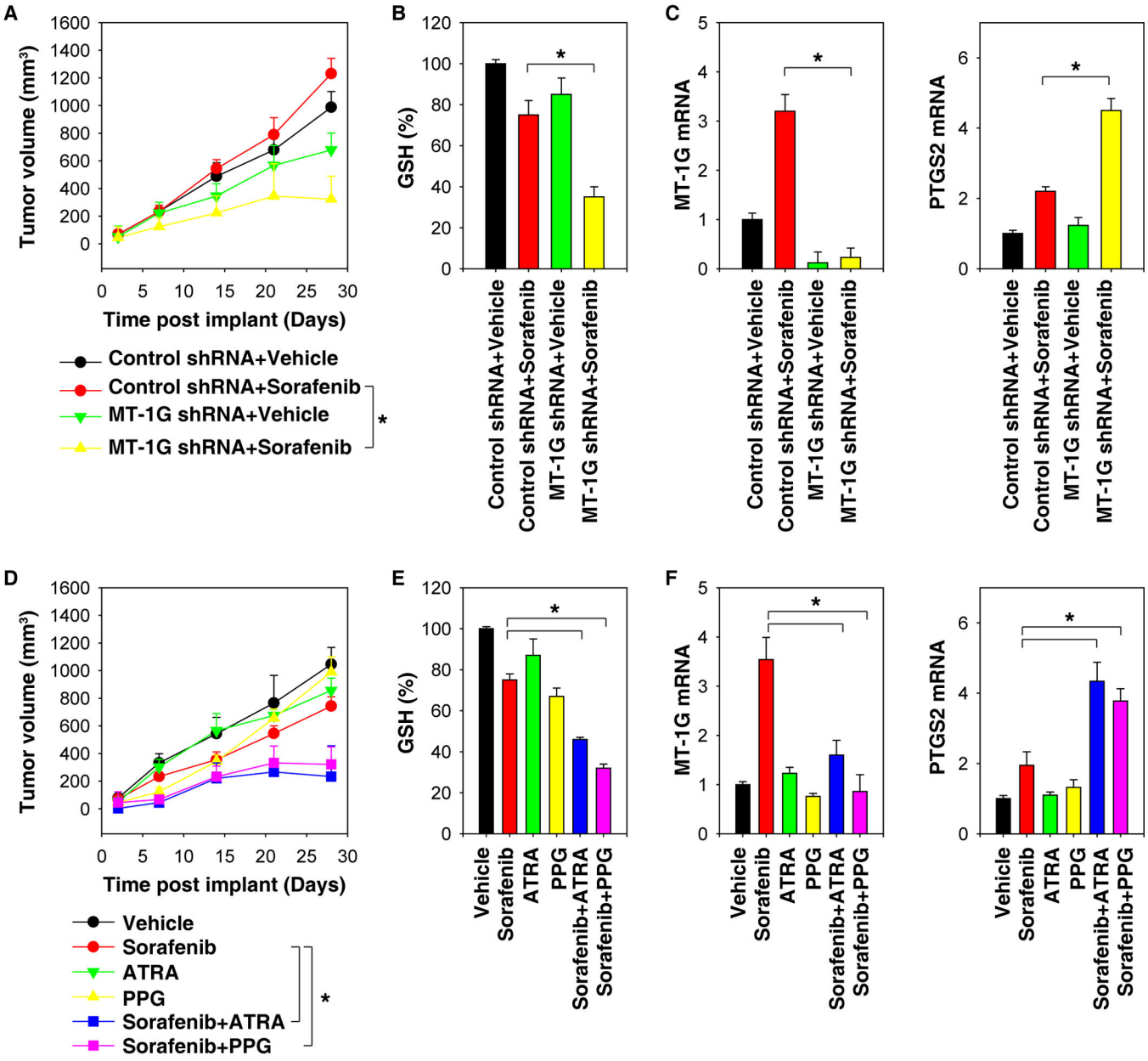

Figure 5. Suppression of metallothionein (MT)-1G enhances the anticancer activity of sorafenib *in vivo*

(A–C) Nude mice were injected subcutaneously with indicated Huh7 cells (2×10^6 cells/mouse) and treated with sorafenib (10 mg/kg/i.p., once every other day) and vehicle at day seven for two weeks (n=5 mice/group). Tumor volume was calculated weekly (A). In parallel, the levels of glutathione (GSH) (B), MT-1G mRNA (C), and prostaglandin-endoperoxide synthase 2 (PTGS2) mRNA (C) in isolated tumor at day 28 were assayed (*$p < 0.05$). (D–F) Nude mice were injected subcutaneously with Huh7 cells (2×10^6 cells/mouse) and treated with sorafenib (10 mg/kg/i.p., once every other day) with or without all-trans retinoic acid (ATRA) (0.5 mg/kg/i.p., once every other day) or propargylglycine (PPG) (10 mg/kg/i.p., once every other day) at day seven for two weeks (n=5 mice/group). Tumor

volume was calculated weekly (E). In parallel, the levels of GSH (E), MT-1G mRNA (F), and PTGS2 mRNA (F) in isolated tumor at day 28 were assayed (*$p < 0.05$).